CHEMPHYSCHEM

Supporting Information

Cross-Polarization Electron-Nuclear Double Resonance Spectroscopy

Roberto Rizzato[a] and Marina Bennati*[a, b]

cphc_201500938_sm_miscellaneous_information.pdf

SI1: Theoretical description of electron nuclear cross-polarization and experimental validation using malonic acid radical single crystal.

The eNCP process can be described by a doubly rotating (mw and rf) frame Hamiltonian using a convenient fictitious spin-half formalism[1]:

$$\tilde{H}_{CP} = \left(\Delta\omega_e - \frac{A}{2}\right) I_z^{1-3} + \omega_{1e} I_x^{1-3} + \left(\Delta\omega_e + \frac{A}{2}\right) I_z^{2-4} + \omega_{1e} I_x^{2-4} - \Delta\omega_n (I_z^{1-2} + I_z^{3-4}) + \omega_{1n} (I_x^{1-2} + I_x^{3-4}) \quad (1)$$

where A is the hyperfine constant, $\Delta\omega_e = \omega_{mw} - \omega_e$ and $\Delta\omega_n = \omega_{rf} - \omega_n$ are the electron and nuclear off-resonance values and ω_{1e}, ω_{1n} the mw and rf field strengths, respectively. The Hamiltonian has been derived specifically for an $\{e - {}^1H\}$ two-spin system considering as spin states in the laboratory frame:

$$|1\rangle = |\beta_e \alpha_n\rangle;\ |2\rangle = |\beta_e \beta_n\rangle;\ |3\rangle = |\alpha_e \alpha_n\rangle;\ |4\rangle = |\alpha_e \beta_n\rangle \quad (2)$$

Such a Hamiltonian is very similar to what derived in ref. [1b] except that we took into account the opposite sign of electron and proton magnetic moments in all terms.

In the typical ENDOR conditions the hyperfine couplings are in the MHz range and the rf field strengths are three orders of magnitude smaller, therefore we assume that $\omega_{1n} \ll A$ and the nuclear spin quantization axis lies along the *z-axis.*

In order to derive the CP conditions, we perform a transformation $U^{-1}\tilde{H}_{CP}U$ that tilts the direction of the "*z*" operators to make them coincident with the effective magnetic fields in each of the electron manifolds, as illustrated below. To this purpose we use the unitary operator: $= [U_y^{1-3}(\varphi_\alpha) U_y^{2-4}(\varphi_\beta)] = e^{-i\varphi_\alpha I_y^{1-3}} e^{-i\varphi_\beta I_y^{2-4}}$. The diagonal part of the nuclear Hamiltonian is not affected by such a rotation and stays diagonal contributing to split the energy of the "new" CP eigenstates by a constant nuclear offset $\Delta\omega_n$.

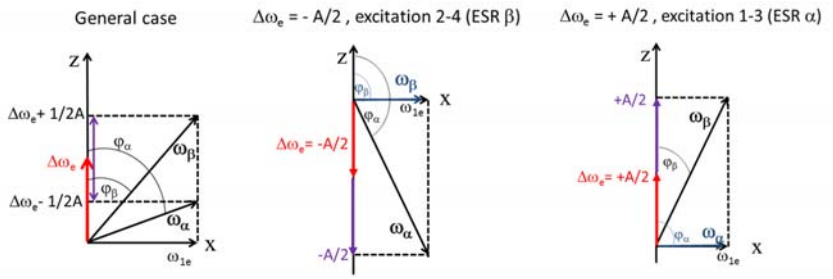

If $A < 0$ we have:

φ_α and φ_β are defined as:

$$\varphi_\alpha = \tan^{-1}\left(\frac{\omega_{1e}}{\Delta\omega_e - \frac{A}{2}}\right) \qquad \varphi_\beta = \tan^{-1}\left(\frac{\omega_{1e}}{\Delta\omega_e + \frac{A}{2}}\right)$$

for $\Delta\omega_e - \frac{A}{2} \geq 0$ otherwise: for $\Delta\omega_e + \frac{A}{2} \geq 0$ otherwise:

$$\varphi_\alpha = \pi + \tan^{-1}\left(\frac{\omega_{1e}}{\Delta\omega_e - \frac{A}{2}}\right) \qquad \varphi_\beta = \pi + \tan^{-1}\left(\frac{\omega_{1e}}{\Delta\omega_e + \frac{A}{2}}\right) \tag{3}$$

The Hamiltonian in such a "tilted" frame gets the form:

$$\mathcal{H}' = \begin{pmatrix} -\frac{1}{2}\omega_\alpha - \frac{\Delta\omega_n}{2} & \omega_{1n}cos(\frac{\varphi_\beta}{2} - \frac{\varphi_\alpha}{2}) & 0 & \omega_{1n}sin(\frac{\varphi_\beta}{2} - \frac{\varphi_\alpha}{2}) \\ \omega_{1n}cos(\frac{\varphi_\beta}{2} - \frac{\varphi_\alpha}{2}) & -\frac{1}{2}\omega_\beta + \frac{\Delta\omega_n}{2} & \omega_{1n}sin(\frac{\varphi_\beta}{2} - \frac{\varphi_\alpha}{2}) & 0 \\ 0 & \omega_{1n}sin(\frac{\varphi_\beta}{2} - \frac{\varphi_\alpha}{2}) & +\frac{1}{2}\omega_\alpha - \frac{\Delta\omega_n}{2} & \omega_{1n}cos(\frac{\varphi_\beta}{2} - \frac{\varphi_\alpha}{2}) \\ \omega_{1n}sin(\frac{\varphi_\beta}{2} - \frac{\varphi_\alpha}{2}) & 0 & \omega_{1n}cos(\frac{\varphi_\beta}{2} - \frac{\varphi_\alpha}{2}) & +\frac{1}{2}\omega_\beta + \frac{\Delta\omega_n}{2} \end{pmatrix} \tag{4}$$

The result is a Hamiltonian with a set of off-diagonal terms proportional to the rf field strength ω_{1n} and which connect couples of diagonal elements such as: $\mathcal{H}'_{1,2}, \mathcal{H}'_{3,4}, \mathcal{H}'_{1,4}, \mathcal{H}'_{2,3}$. When the difference between a pair of diagonal elements become of the order of ω_{1n}, these connecting elements become significant and may efficiently drive a transition between two CP states. By applying a finite nuclear offset $\Delta\omega_n$, the magnetic interaction along the z-axis which is "felt" by the nuclear spins is modulated and the energy levels are perturbed accordingly. In this way, degeneracies can be generated at any time by setting the rf to a value of $\Delta\omega_n$ such that a CP condition is fulfilled.

Such matching conditions are summarized as following:

$$\begin{aligned} E_{|1'\rangle} - E_{|2'\rangle} = 0 \;\rightarrow\; \Delta\omega_n = -\frac{1}{2}(\omega_\alpha - \omega_\beta) \\ E_{|3'\rangle} - E_{|4'\rangle} = 0 \;\rightarrow\; \Delta\omega_n = +\frac{1}{2}(\omega_\alpha - \omega_\beta) \\ E_{|1'\rangle} - E_{|4'\rangle} = 0 \;\rightarrow\; \Delta\omega_n = -\frac{1}{2}(\omega_\alpha + \omega_\beta) \\ E_{|2'\rangle} - E_{|3'\rangle} = 0 \;\rightarrow\; \Delta\omega_n = +\frac{1}{2}(\omega_\alpha + \omega_\beta) \end{aligned} \tag{5}$$

where $\omega_\alpha = \sqrt{\left(-\Delta\omega_e + \frac{A}{2}\right)^2 + \omega_{1e}^2}$, $\omega_\beta = \sqrt{\left(-\Delta\omega_e - \frac{A}{2}\right)^2 + \omega_{1e}^2}$.

We note here that, the signs in the expressions of $\omega_{\alpha,\beta}$ are different from what derived in ref. [1b], but this is again due to considering the specific case of an electron-proton spin system allowing us to correctly describe the experimental observations.

The efficiency of the polarization transfer between the electron and the nucleus at each CP condition is determined by the magnitudes of the off-diagonal elements. These depend on the excitation conditions, i.e. electron offset $\Delta\omega_e$, mw field strength ω_{1e} and hyperfine coupling *A*.

However, in order to evaluate the effect that a matched CP condition has on the polarization of the spin system and ultimately on the ENDOR spectrum, we have to analyze the evolution of spin populations during the CP step. The density matrix formalism allows to illustrate the effect that each of the four CP transitions have after a time t_{CP} in the tilted frame and back in the rotating frame at a time t_{ENDOR} which corresponds to the ENDOR detection. As an example we will refer to the case of excitation of the β–line in the EPR spectrum (transition [2-4]) and negative hyperfine constant as in the case of malonic acid.

The thermal equilibrium density matrix $\hat{\rho}(eq)$ in the doubly rotating frame, ignoring the initial nuclear magnetization has the form:

$$\hat{\rho}(eq) = \frac{1}{2}\hat{1} + \frac{1}{2}\mathbb{B}_s\hat{S}_z = \frac{1}{2}\hat{1} + \frac{1}{2}\mathbb{B}_s[-I_z^{1-3} - I_z^{2-4}] \tag{6}$$

where $\mathbb{B}_s$ is the electron Boltzmann factor. (For clarity we will drop the first term $\frac{1}{2}\hat{1}$ presuming its presence in each of the following density matrix expressions.)

However it is helpful to utilize a more general form that represents the spin system at the starting point of the CP process and separates the electron polarizations of the α and β electron manifolds.

Thus we may write eq. (6) as:

$$\hat{\rho}(0) = \boldsymbol{R}[-I_z^{1-3} - I_z^{2-4}] = R_\alpha[-I_z^{1-3}] + R_\beta[-I_z^{2-4}] \tag{7}$$

Where $R_{\alpha,\beta}$ are polarization factors proportional to the projection of the magnetization vector onto the effective field for each of the α and β electron manifold respectively.

When EPR excitation occurs by means of a $(\frac{\pi}{2})_y$ mw pulse and on resonance with the [2-4] transition:

$$\hat{\rho}(0^+) = +R_\beta[-I_x^{2-4}] + R_a[-I_z^{1-3}] \tag{8}$$

The $\frac{\pi}{2}$ pulse tilts the magnetization of the β-manifold onto the x-y plane and, under the approximation of selective pulse ($\omega_{1e} \ll |A|$) on resonance with the [2-4] EPR transition, the α-manifold stays almost unperturbed. Immediately after the first $\frac{\pi}{2}$ pulse, the spinlock pulse locks the magnetization of the β-manifold along the effective field ω_β which is in the x-y plane and the magnetization of the α-manifold keeps staying almost unaltered due to strong off-resonance field.

In order to describe the spin dynamics during CP, it's convenient to transform $\hat{\rho}(0^+)$ to the tilted frame:

$$\hat{\rho}^T(0^+) = U^{-1}\hat{\rho}(0^+)U = e^{-i\varphi_\alpha I_y^{1-3}} e^{-i\varphi_\beta I_y^{2-4}} \{R_\beta[-I_x^{2-4}] + R_a[-I_z^{1-3}]\} e^{i\varphi_\alpha I_y^{1-3}} e^{i\varphi_\beta I_y^{2-4}} \quad (9)$$
$$= R_\alpha cos\varphi_\alpha[-I_z^{1-3}] + R_\alpha sin\varphi_\alpha[-I_x^{1-3}] + R_\beta cos\varphi_\beta[-I_x^{2-4}] + R_\beta sin\varphi_\beta[I_z^{2-4}]$$

When no CP condition is matched or no rf field is applied, the diagonal elements of $\hat{\rho}^T(0^+)$ stay locked along the lock fields and decay with a characteristic relaxation time $T_{1\rho}$. All other matrix elements decay with a shorter T_{2e} time which is the dephasing time of the magnetization rotating around the lock fields. The actual values of the polarization coefficients of the density matrix elements depend on the mw field strength ω_{1e} , on the mw off-resonance value $\Delta\omega_e$ and the hyperfine interaction *A*.

For [2-4] EPR excitation considering $A < 0$: $\varphi_\alpha \approx 0°$; $\varphi_\beta \approx 90°$

$$\hat{\rho}^T(0^+) = R_\alpha[-I_z^{1-3}] + R_\beta[I_z^{2-4}] = \frac{1}{2}\begin{bmatrix} -R_\alpha \\ R_\beta \\ R_\alpha \\ -R_\beta \end{bmatrix} \quad (10)$$

If, at this stage, rf irradiation is applied with a $\Delta\omega_n$ satisfying a $[i-j]$ CP condition, the density matrix coefficients become time dependent. Oscillation of I_z^{i-j} and $I_{x,y}^{i-j}$ coefficients occurs caused by the corresponding off-diagonal matrix element and after a time t_{CP} they decay to zero because of T_{2e} relaxation. The diagonal elements of the spin states $|i\rangle$ and $|j\rangle$ become equal and the coefficients of I_z^{i-j} vanish.

If [1-2] or [3-4] CP conditions are matched, under the approximation of selective EPR excitation $R_\alpha \approx R_\beta \approx 1/2\langle\hat{S}_z\rangle \equiv R$ we obtain:

$$\hat{\rho}^T(0^+) = \frac{1}{2}\begin{bmatrix} -R \\ R \\ R \\ -R \end{bmatrix} \rightarrow \hat{\rho}_{1-2}^T(t_{CP}) = \frac{1}{2}\begin{bmatrix} \frac{-R+R}{2} \\ \frac{-R+R}{2} \\ R \\ -R \end{bmatrix} = \frac{1}{2}\begin{bmatrix} 0 \\ 0 \\ R \\ -R \end{bmatrix} \quad (11)$$

$$\hat{\rho}_{3-4}^T(t_{CP}) = \frac{1}{2}\begin{bmatrix} -R \\ R \\ \frac{R-R}{2} \\ \frac{R-R}{2} \end{bmatrix} = \frac{1}{2}\begin{bmatrix} -R \\ R \\ 0 \\ 0 \end{bmatrix} \quad (12)$$

This is equivalent to:

$$\hat{\rho}_{1-2}^T(t_{CP}) = -\frac{R}{2}[I_z^{1-3}] + \frac{R}{2}[I_z^{2-4}] + \frac{R}{2}[I_z^{1-2} + I_z^{3-4}]$$
$$\hat{\rho}_{3-4}^T(t_{CP}) = -\frac{R}{2}[I_z^{1-3}] + \frac{R}{2}[I_z^{2-4}] - \frac{R}{2}[I_z^{1-2} + I_z^{3-4}] \quad (13)$$

To determine the polarization distribution of the spin system at the end of the CP-step we have to transform $\hat{\rho}^T(t)$ back to the doubly rotating frame by means of the unitary transformation: $\hat{\rho}(t_{CP}) = U\hat{\rho}^T_{1-2(3-4)}(t_{CP})U^{-1}$. Thus we obtain:

$$\begin{aligned}
\hat{\rho}_{1-2}(t_{CP}) &= -\frac{R}{2}[I_z^{1-3}] - \frac{R}{2}[I_x^{2-4}] + \frac{R}{2}[I_z^{1-2} + I_z^{3-4}] \longrightarrow \hat{\rho}_{1-2}(t_{ENDOR}) = \frac{1}{2}\begin{bmatrix}\begin{bmatrix} 0 \\ -R/2 \\ +R \\ -R/2 \end{bmatrix}\end{bmatrix} \\
\hat{\rho}_{3-4}(t_{CP}) &= -\frac{R}{2}[I_z^{1-3}] - \frac{R}{2}[I_x^{2-4}] - \frac{R}{2}[I_z^{1-2} + I_z^{3-4}] \longrightarrow \hat{\rho}_{3-4}(t_{ENDOR}) = \frac{1}{2}\begin{bmatrix}\begin{bmatrix} -R \\ +R/2 \\ 0 \\ +R/2 \end{bmatrix}\end{bmatrix}
\end{aligned} \tag{14}$$

The polarization coefficients corresponding to the diagonal elements of $\hat{\rho}_{1-2(3-4)}(t_{CP})$ will all contribute to the intensity of the CP-ENDOR spectrum, whereas the polarization of the off-diagonal term I_x^{2-4} is what we refocus and detect in an eNCP experiment by setting a mw π pulse after a time $t_{eNCP} < T_{2e}$. It's worth to note that the net depletion of the signal that we detect in such an experiment in coincidence with a matched CP condition is direct consequence of the decrease of the polarization coefficient of the term I_x^{2-4} with respect to eq. (8). We can now determine the ENDOR signal considering it as proportional to the population differences between corresponding density matrix elements. ENDOR signal can be defined as the difference of the EPR signal intensity with and without rf irradiation on resonance with nuclear (1-2) and (3-4) ENDOR transitions.

For selective detection on the [2-4] EPR transition and selective rf on resonance with (1-2):

$$S_{CP[1-2]}^{ENDOR(1-2)} \sim (\rho_{22} - \rho_{44}) - (\rho_{11} - \rho_{44}) = \rho_{22} - \rho_{11} = -\frac{1}{4}R \tag{15}$$

For selective EPR detection on the [2-4] transition and selective rf on resonance with (3-4):

$$S_{CP[1-2]}^{ENDOR(3-4)} \sim (\rho_{22} - \rho_{44}) - (\rho_{22} - \rho_{33}) = \rho_{33} - \rho_{44} = +\frac{3}{4}R \tag{16}$$

Whereas in the case of CP [3-4]

$$S_{CP[3-4]}^{ENDOR(1-2)} \sim \rho_{22} - \rho_{11} = +\frac{3}{4}R \tag{17}$$

$$S_{CP[3-4]}^{ENDOR(3-4)} \sim \rho_{33} - \rho_{44} = -\frac{1}{4}R \tag{18}$$

On the other hand, matched [1-4] and [2-3] CP conditions do not produce any net effect on the density matrix:

$$\hat{\rho}^T(0^+) = \frac{1}{2}\begin{bmatrix}\begin{bmatrix}-R\\R\\R\\-R\end{bmatrix}\end{bmatrix} \rightarrow \hat{\rho}^T_{1-4}(t_{CP}) = \frac{1}{2}\begin{bmatrix}\begin{bmatrix}\frac{-R-R}{2}\\R\\R\\\frac{-R-R}{2}\end{bmatrix}\end{bmatrix} = \frac{1}{2}\begin{bmatrix}\begin{bmatrix}-R\\R\\R\\-R\end{bmatrix}\end{bmatrix} \tag{19}$$

$$\hat{\rho}^T_{2-3}(t_{CP}) = \frac{1}{2}\begin{bmatrix}\begin{bmatrix}-R\\\frac{R+R}{2}\\\frac{R+R}{2}\\-R\end{bmatrix}\end{bmatrix} = \frac{1}{2}\begin{bmatrix}\begin{bmatrix}-R\\R\\R\\-R\end{bmatrix}\end{bmatrix} \tag{20}$$

Therefore in the rotating frame we obtain:

$$\hat{\rho}_{1-4}(t_{CP}) = \hat{\rho}_{2-3}(t_{CP}) = -R[I_z^{1-3}] - R[I_x^{2-4}] \tag{21}$$

which is in fact equivalent to eq. (8)

Thus, after decay of coherences: $\hat{\rho}_{1-4}(t_{ENDOR}) = \frac{1}{2}\begin{bmatrix}\begin{bmatrix}-R\\0\\+R\\0\end{bmatrix}\end{bmatrix}$, which results in the following ENDOR signals:

$$\begin{aligned} S^{ENDOR(1-2)}_{CP[1-4],[2-3]} &\sim \rho_{22} - \rho_{11} = +\frac{1}{2}R \\ S^{ENDOR(3-4)}_{CP[1-4],[2-3]} &\sim \rho_{33} - \rho_{44} = +\frac{1}{2}R \end{aligned} \tag{22}$$

In Table S1 signal intensities of CP-ENDOR spectra are summarized for all possible cases of EPR excitation and CP conditions, as well as for positive and negative hyperfine coupling constant.

	$A > 0$				$A < 0$			
	EPR α		EPR β		EPR α		EPR β	
	hf line 1→2	hf line 3→4	hf line 1→2	hf line 3→4	hf line 1→2	hf line 3→4	hf line 1→2	hf line 3→4
CP [1-4]	½ R	½ R	¾ R	- ¼ R	- ¼ R	¾ R	½ R	½ R
CP [2-3]	½ R	½ R	- ¼ R	¾ R	¾ R	- ¼ R	½ R	½ R
CP [1-2]	- ¼ R	¾ R	½ R	½ R	½ R	½ R	- ¼ R	¾ R
CP [3-4]	¾ R	- ¼ R	½ R	½ R	½ R	½ R	¾ R	- ¼ R

Table S1 Theoretical signal intensities of CP-ENDOR obtained by the density matrix treatment.

We conclude that, although in principle all 4 matching conditions are allowed, they have a different effect on the polarization of the system. Fig. S1 shows experimental evidence on how CP transitions are effective in pairs according as we excite one or the other EPR line.

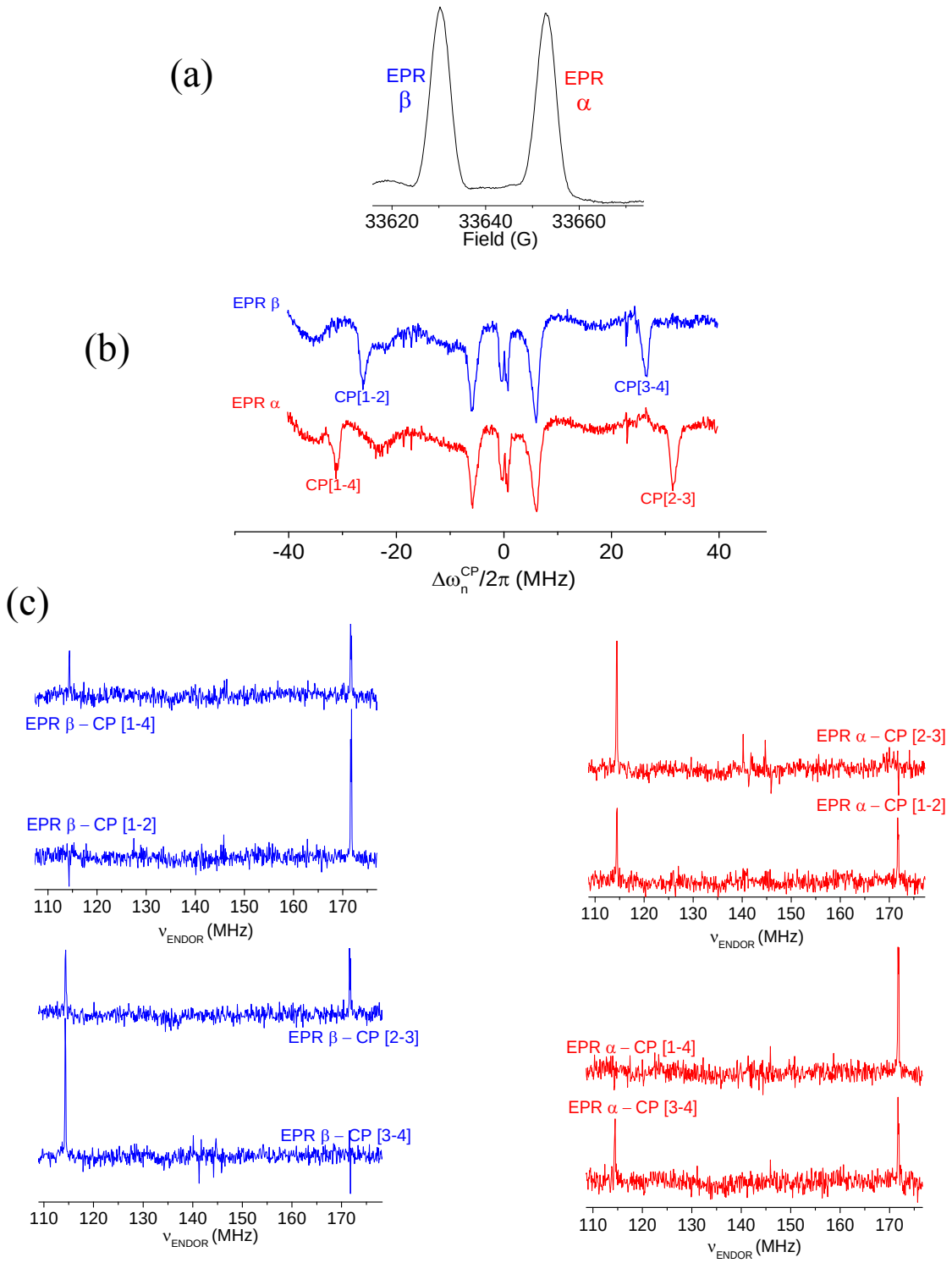

Fig. S1 EPR (a), eNCP (b) and CP-ENDOR (c) spectra of malonic acid radical single crystal at ν_{EPR} = 94 GHz and T = 30 K. eNCP spectra are reported for excitation of the EPR-β transition (blue line) and EPR-α transition (red line). The assignment of the CP conditions has been done according to eq.

(5) and considering the experimental parameters: A = - 58 MHz, $\omega_{1e}/2\pi$ = 6 MHz, $\Delta\omega_e/2\pi$ = ± 29 MHz. For both eNCP and CP-ENDOR experiments CP pulse length was 200 μs. Other parameters are reported in caption of Fig. 2 in the main text.

SI2. Effect of EPR excitation frequency on eNCP spectra

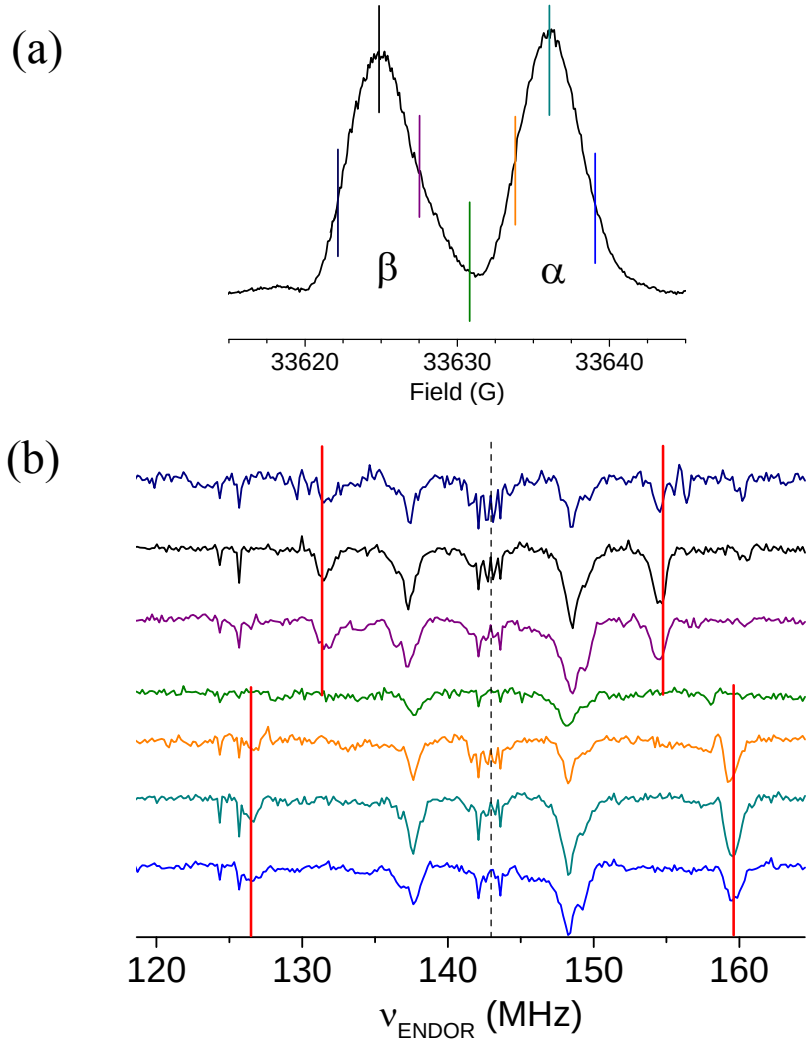

Fig. S2 eNCP Spectra (b) as a function of the mw excitation in the EPR line (a) of malonic acid radical single crystal. Color bars over the EPR spectrum in (a) correspond to field points utilized in (b) Exp. conditions : ν_{EPR} = 94 GHz, T = 20 K, repetition time 350 ms, 1 shot per point, 300 points, 80 scans per spectrum, $\pi/2_{MW}$ = 30 ns, ω_{1e} = 8 MHz , CP pulse length = 100 us, $\Delta\omega_n^{CP}$ is swept.

SI3. Line shape of CP-ENDOR spectra obtained with different CP offsets

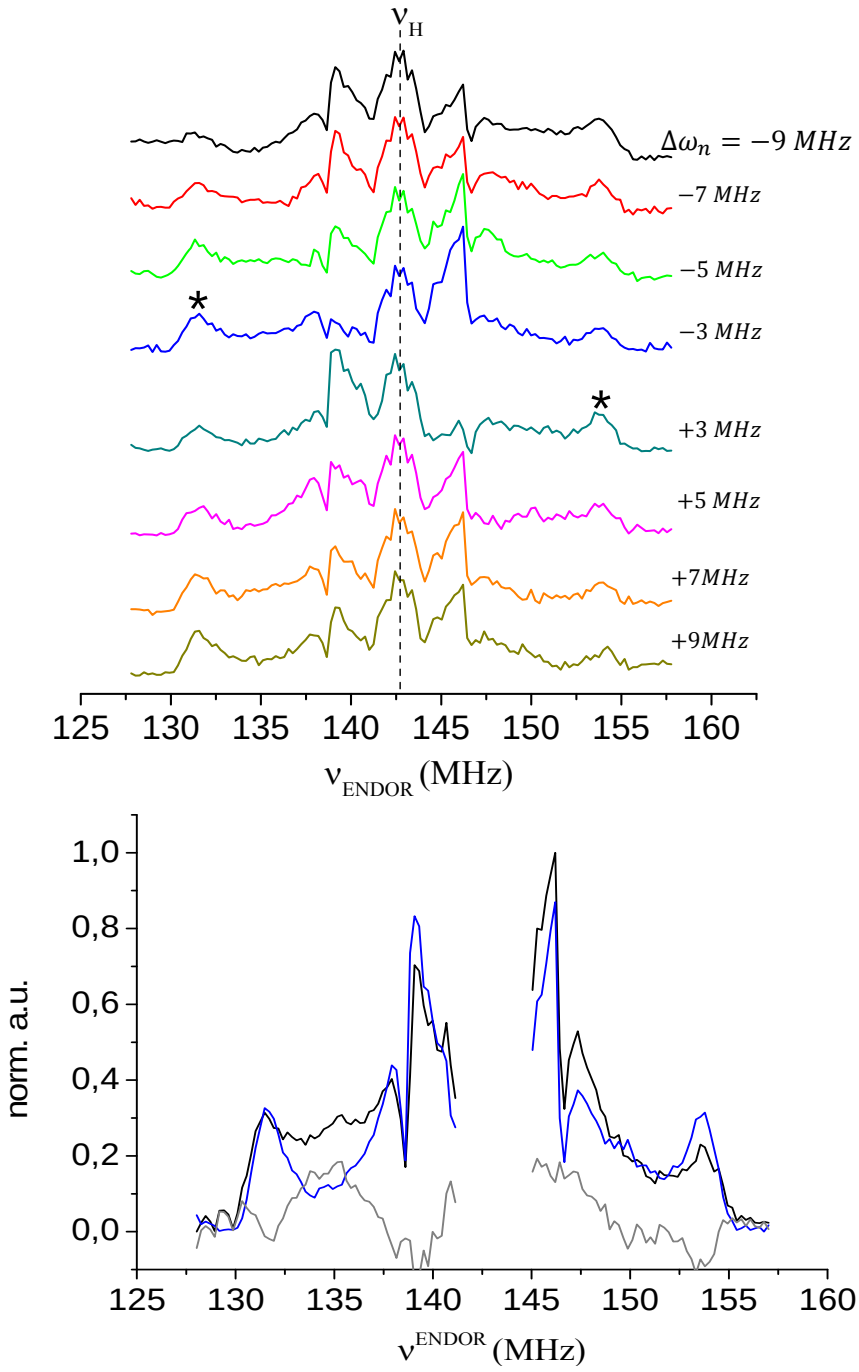

Fig. S3 CP-ENDOR and Davies spectra of Y_{122}• in RNR at T = 10 K. Top: CP ENDOR spectra at different CP frequencies according to Fig. 4 in the main text. The asterisks on the blue and the cyan spectra indicate an effect also on the small coupling corresponding to the 3-5 protons in Y_{122}• although CP condition for the 2-6 protons coupling at ~ 7 MHz was matched. Bottom: comparison of Davies ENDOR spectrum (black line) and the sum of eight single CP-ENDOR spectra (blue line); residual difference (gray line). A more quantitative comparison of the line shape has been perfomed by evaluating the root mean square deviation RMSD = 0.08 between the two spectra.

SI4. CP-ENDOR in two dimensions

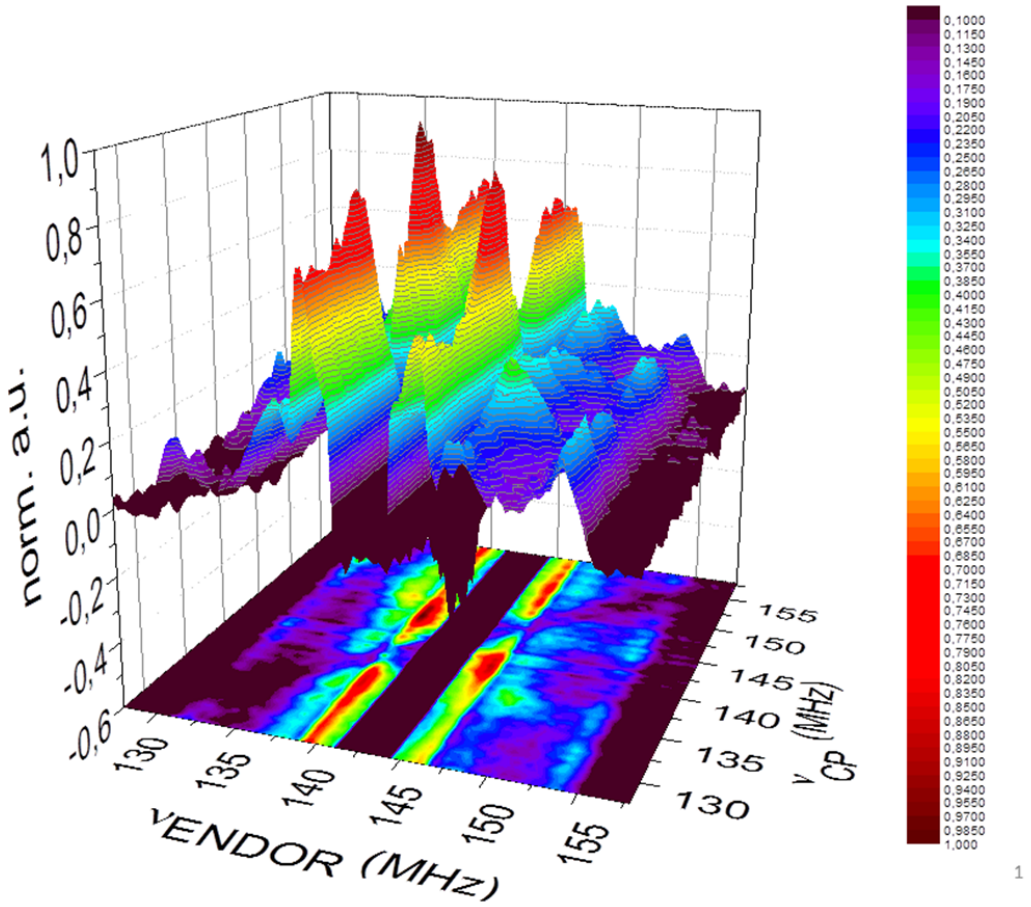

Fig. S4 CP-ENDOR spectrum recorded as a function of the π - ENDOR pulse frequency (first dimension) and of the CP rf-offset (second dimension) of tyrosyl radical Y122* in *E. coli* ribonucleotide reductase. mw power was $\omega 1e/2\pi$ = 1.2 MHz, t_{CP} = 200 µs. The ENDOR-rf (x-axis) was swept using random acquisition modus, 1 shot/point, recording 128 points with a repetition time T_r = 300 ms. The CP-rf (y-axis) was swept sequentially pumping rf at 64 different values in a range of 30 MHz. 22 scans of the whole 2D spectrum have been accumulated.

SI5. Comparison of CP-ENDOR and Davies line shapes

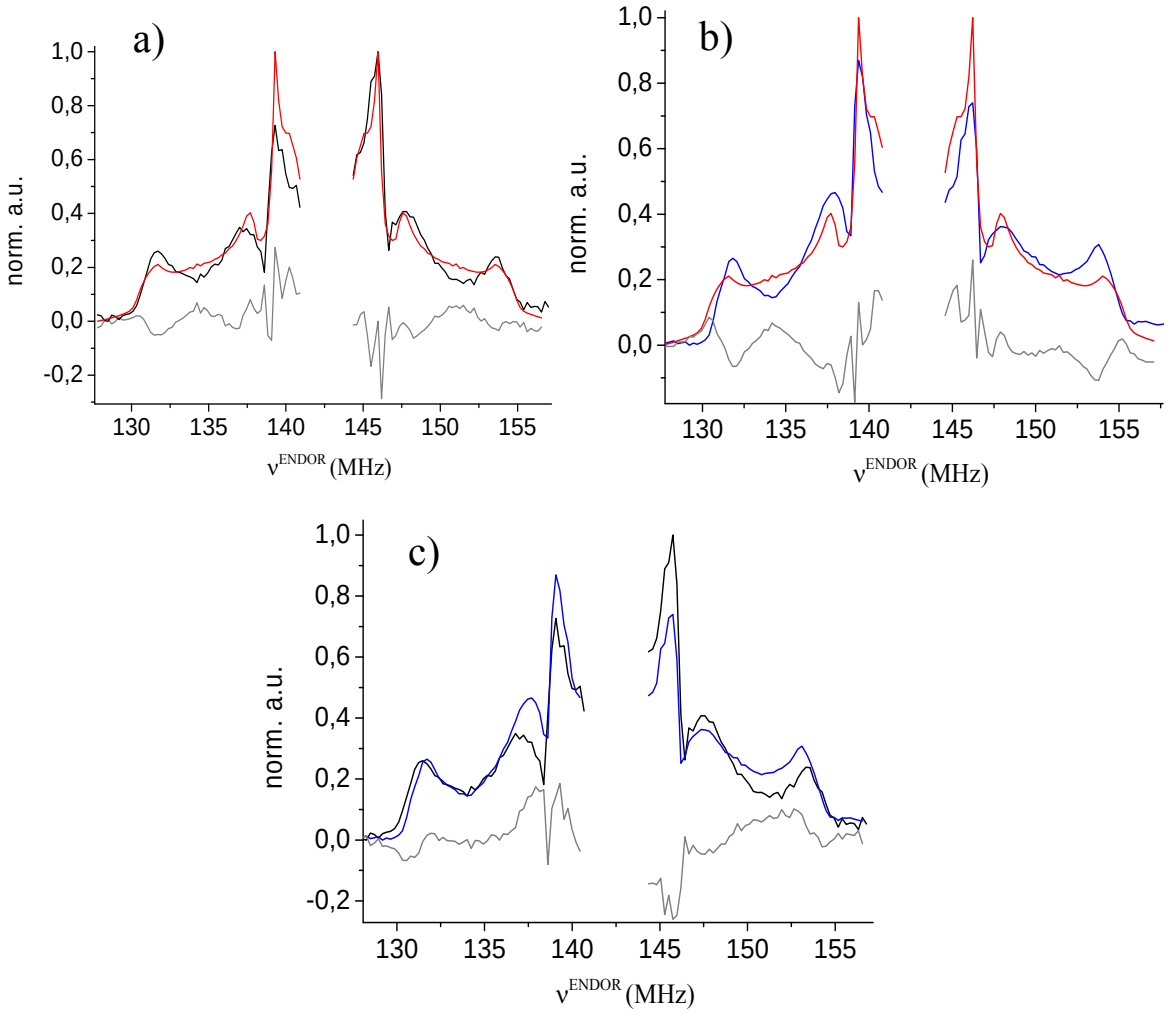

Fig. S5 Comparison of line shapes for CP-ENDOR and Davies spectra of Y_{122}• in RNR at T = 5 K. a) Davies ENDOR spectrum (black line), simulation of ENDOR spectrum (red line), residual difference (gray line), RMSD = 0.065; b) pseudo-2D ENDOR spectrum (blue line), simulation of ENDOR spectrum (red line), residual difference (gray line), RMSD = 0.069; c) pseudo-2D ENDOR spectrum (blue line), Davies ENDOR spectrum (black line), residual difference (gray line), RMSD = 0.079. A quantitative comparison of the line shapes has been performed by evaluating the root mean square deviation (RMSD) between the experimental spectra and the simulation.

SI6. Parameters for simulation of the Davies ENDOR spectrum

The ENDOR spectrum has been computed using a Matlab code previously developed in house[2]. The program simulates the EPR powder spectrum starting from the experimental g-tensor and a set of hyperfine couplings. The orientations within the pulse excitation profile at a certain field are extracted and the ENDOR frequencies are calculated to the first order. The ENDOR spectrum is then convoluted with a preparation function. The matrix peak is simulated by a Gaussian function and weighted to obtain the observed intensity.

Protons	A_x (MHz)	A_y (MHz)	A_z (MHz)	α (deg)	β (deg)	γ (deg)
3 or 5	-26.0	-9.5	-19.0	25	0	0
3 or 5	-26.0	-9.5	-19.0	25	0	0
β_1	58.0	55.4	52.4	0	0	0
β_2	2.0	7.4	-0.9	60	-8	-90
2 or 6	7.0	7.1	2.1	205	0	0
2 or 6	7.0	7.1	2.1	-205	0	0

Table S2 Hyperfine Tensor parameters used for simulating the ENDOR spectrum reported in Fig. S5 and Fig. 5 in the main text.

References

[1] a) S. Vega, *J.Chem. Phys.* **1978**, *68*;
b) R. Rizzato, I. Kaminker, S. Vega, M. Bennati, *Mol. Phys.* **2013**, *111*, 2809-2823.

[2] M. Bennati, C. Farrar, J. Bryant, S. Inati, V. Weis, G. Gerfen, P. Riggs-Gelasco, J. Stubbe, R. G. Griffin, *J. Magn. Reson.* **1999**, *132*, 232-243.